The Big-Bang Nucleosynthesis (BBNS) within the Scale-Invariant Vacuum (SIV) paradigm

Vesselin G. Gueorguiev[1,2] and Andre Maeder[3]

[1] *Institute for Advanced Physical Studies (IAPS), Sofia, Bulgaria,*
[2] *Ronin Institute for Independent Scholarship, Montclair, NJ, USA,*
[3] *Geneva Observatory, Geneva, Switzerland.*

Week 3 Workshop of the program INT-24-3 on
Quantum Few- and Many-Body Systems in Universal Regimes,
INT, Seattle, WA, USA

Outline

1. Motivation - Einstein GR, Weyl Geometry, and SIV
2. Background - standard BBNS and the SIV analytic expressions
3. Method - values of $a(T)$, $\tau(T)$, and $\rho(T)$ during the BBNS
4. Results - abundances of the light elements
5. Summary

Einstein GR (EGR) and Weyl Integrable Geometry (WIG) [1, 2, 3]

- Einstein GR guarantees $\delta\left\|\vec{v}\right\| = 0$ along a geodesic.

Q: Could the DM and DE phenomena be artifacts of non-zero $\delta\left\|\vec{v}\right\|$, but often negligible $\delta\left\|\vec{v}\right\| \approx 0$ and almost zero value, that accumulates over cosmic distances?

- In Weyl Integrable Geometry $\oint \delta\left\|\vec{v}\right\| = 0$ along a closed loop - this defeats the Einstein's inital objection!
- Not implementing re-parametrization invariance in a model could lead to un-proper time parametrization [4] that seems to induce "fictitious forces" in the equations of motion similar to the forces derived in the weak field SIV regime.

Einstein GR (EGR) and Weyl Integrable Geometry (WIG) [1, 2, 3]

- Einstein GR guarantees $\delta\|\vec{v}\| = 0$ along a geodesic.

Q: Could the DM and DE phenomena be artifacts of non-zero $\delta\|\vec{v}\|$, but often negligible $\delta\|\vec{v}\| \approx 0$ and almost zero value, that accumulates over cosmic distances?

- In Weyl Integrable Geometry $\oint \delta\|\vec{v}\| = 0$ along a closed loop - this defeats the Einstein's inital objection!
- Not implementing re-parametrization invariance in a model could lead to un-proper time parametrization [4] that seems to induce "fictitious forces" in the equations of motion similar to the forces derived in the weak field SIV regime.

Einstein GR (EGR) and Weyl Integrable Geometry (WIG) [1, 2, 3]

- Einstein GR guarantees $\delta\|\vec{v}\| = 0$ along a geodesic.

Q: Could the DM and DE phenomena be artifacts of non-zero $\delta\|\vec{v}\|$, but often negligible $\delta\|\vec{v}\| \approx 0$ and almost zero value, that accumulates over cosmic distances?

- In Weyl Integrable Geometry $\oint \delta\|\vec{v}\| = 0$ along a closed loop - this defeats the Einstein's inital objection!

- Not implementing re-parametrization invariance in a model could lead to un-proper time parametrization [4] that seems to induce "fictitious forces" in the equations of motion similar to the forces derived in the weak field SIV regime.

Einstein GR (EGR) and Weyl Integrable Geometry (WIG) [1, 2, 3]

- Einstein GR guarantees $\delta\left\|\vec{v}\right\|=0$ along a geodesic.

Q: Could the DM and DE phenomena be artifacts of non-zero $\delta\left\|\vec{v}\right\|$, but often negligible $\delta\left\|\vec{v}\right\|\approx 0$ and almost zero value, that accumulates over cosmic distances?

- In Weyl Integrable Geometry $\oint\delta\left\|\vec{v}\right\|=0$ along a closed loop - this defeats the Einstein's inital objection!

- Not implementing re-parametrization invariance in a model could lead to un-proper time parametrization [4] that seems to induce "fictitious forces" in the equations of motion similar to the forces derived in the weak field SIV regime.

SIV based Cosmology: first in 1977 by Canuto et al. [3] then in 2017 by Maeder [6]

$$g'_{\mu\nu} = \lambda g_{\mu\nu}$$

The FLRW equations within the Weyl Integrable Geometry:

$$\frac{8\pi G\rho}{3} = \frac{k}{a^2} + \frac{\dot{a}^2}{a^2} + 2\frac{\dot{\lambda}\,\dot{a}}{\lambda\, a} + \frac{\dot{\lambda}^2}{\lambda^2} - \frac{\Lambda_{\mathrm{E}}\lambda^2}{3}, \tag{1}$$

$$-8\pi Gp = \frac{k}{a^2} + 2\frac{\ddot{a}}{a} + 2\frac{\ddot{\lambda}}{\lambda} + \frac{\dot{a}^2}{a^2} + 4\frac{\dot{a}\,\dot{\lambda}}{a\,\lambda} - \frac{\dot{\lambda}^2}{\lambda^2} - \Lambda_{\mathrm{E}}\,\lambda^2. \tag{2}$$

In SIV gauge, $\lambda = t_0/t$, **the cosmological constant disappears**:

$$\frac{8\pi G\rho}{3} = \frac{k}{a^2} + \frac{\dot{a}^2}{a^2} + 2\frac{\dot{a}\dot{\lambda}}{a\lambda}, \tag{3}$$

$$-8\pi Gp = \frac{k}{a^2} + 2\frac{\ddot{a}}{a} + \frac{\dot{a}^2}{a^2} + 4\frac{\dot{a}\dot{\lambda}}{a\lambda}. \tag{4}$$

Where the Scale Invariant Vacuum (SIV) idea has been applied? [5]

- Today: Primordial Nucleosynthesis within the SIV paradigm.

✓ The SIV cosmology **is a viable alternative to ΛCDM.**
  - In the SIV gauge the cosmological constant **disappears**.
  - Diminishing differences for higher densities ($\lambda \to 1$) [6, 7].

✓ Radial Acceleration Relation (RAR) for dwarf spheroidals [8].

✓ SIV has fast enough growth of the density fluctuations [9].

✓ **Early inflation is natural** within the SIV cosmology [10]!
  - SIV exhibits a graceful exit from inflation.

Where the Scale Invariant Vacuum (SIV) idea has been applied? [5]

- Today: Primordial Nucleosynthesis within the SIV paradigm.

✓ The SIV cosmology **is a viable alternative to ΛCDM.**
  - In the SIV gauge the cosmological constant **disappears**.
  - Diminishing differences for higher densities ($\lambda \to 1$) [6, 7].

✓ Radial Acceleration Relation (RAR) for dwarf spheroidals [8].

✓ SIV has fast enough growth of the density fluctuations [9].

✓ **Early inflation is natural** within the SIV cosmology [10]!
  - SIV exhibits **a graceful exit from inflation**.

The time variable τ is obtained from the FLRW equation

$$\dot{a}/a = H = \sqrt{\frac{8}{3}\pi G\rho(a)} \Rightarrow \ \tau(a)\ ,\ \text{while}\ a(T) = a_0 T_0/(T S^{1/3}).$$

The usual reaction rates for production and reduction of a nucleus are re-expressed from the traditional reaction form $i+j \leftrightarrow k+l$ (P131) into a new form (P136) using $Y_i = n_i/n_b$ where Γ-s are in units of s^{-1}:

$$(P131) \quad \dot{n}_i \supset n_k n_l \gamma_{kl\to ij} - n_i n_j \gamma_{ij\to kl}\,, \qquad \gamma_{ij\to kl} = \langle \sigma v\rangle_{ij\to kl}\,, \ (P132)$$
$$(P136) \quad \dot{Y}_i \supset Y_k Y_l \Gamma_{kl\to ij} - Y_i Y_j \Gamma_{ij\to kl}, \qquad \Gamma_{ij\to kl} = n_b \gamma_{ij\to kl}\,. \quad (P137)$$

Here, the standard reaction rate $\gamma_{j\ldots\to i\ldots}$ is in units cm^3/s.

Based on (P136), one has for the transition from EGR to WIG (SIV):

$$\frac{dY_i}{d\tau'} = Y_k Y_l \Gamma'_{kl\to ij} - Y_i Y_j \Gamma'_{ij\to kl}, \Rightarrow \frac{1}{\lambda}\frac{dY_i}{d\tau} = Y_k Y_l \Gamma'_{kl\to ij} - Y_i Y_j \Gamma'_{ij\to kl},$$

where $d\tau' = \lambda\, d\tau$ based on the EGR↔WIG (SIV) relation $g'_{\mu\nu} = \lambda^2 g_{\mu\nu}$.

The time variable τ is obtained from the FLRW equation

$$\dot{a}/a = H = \sqrt{\frac{8}{3}\pi G\rho(a)} \Rightarrow \tau(a)\text{ , while } a(T) = a_0 T_0/(T\, S^{1/3}).$$

The usual reaction rates for production and reduction of a nucleus are re-expressed from the traditional reaction form $i+j \leftrightarrow k+l$ (P131) into a new form (P136) using $Y_i = n_i/n_b$ where Γ-s are in units of s^{-1}:

$$(P131) \quad \dot{n}_i \supset n_k n_l \gamma_{kl\to ij} - n_i n_j \gamma_{ij\to kl}\,, \qquad \gamma_{ij\to kl} = \langle \sigma v\rangle_{ij\to kl}\,, \; (P132)$$

$$(P136) \quad \dot{Y}_i \supset Y_k Y_l \Gamma_{kl\to ij} - Y_i Y_j \Gamma_{ij\to kl}, \qquad \Gamma_{ij\to kl} = n_b \gamma_{ij\to kl}\,. \quad (P137)$$

Here, the standard reaction rate $\gamma_{j\ldots\to i\ldots}$ is in units cm^3/s.

Based on (P136), one has for the transition from EGR to WIG (SIV):

$$\frac{dY_i}{d\tau'} = Y_k Y_l \Gamma'_{kl\to ij} - Y_i Y_j \Gamma'_{ij\to kl}, \Rightarrow \frac{1}{\lambda}\frac{dY_i}{d\tau} = Y_k Y_l \Gamma'_{kl\to ij} - Y_i Y_j \Gamma'_{ij\to kl},$$

where $d\tau' = \lambda\, d\tau$ based on the EGR$\leftrightarrow$WIG (SIV) relation $g'_{\mu\nu} = \lambda^2 g_{\mu\nu}$.

The time variable τ is obtained from the FLRW equation

$$\dot{a}/a = H = \sqrt{\frac{8}{3}\pi G\rho(a)} \Rightarrow \tau(a)\,, \text{ while } a(T) = a_0 T_0/(T\,S^{1/3}).$$

The usual reaction rates for production and reduction of a nucleus are re-expressed from the traditional reaction form $i + j \leftrightarrow k + l$ (P131) into a new form (P136) using $Y_i = n_i/n_b$ where Γ-s are in units of s^{-1}:

$$\begin{aligned} &(P131) \quad \dot{n}_i \supset n_k n_l \gamma_{kl\to ij} - n_i n_j \gamma_{ij\to kl}\,, \qquad \gamma_{ij\to kl} = \langle \sigma v \rangle_{ij\to kl}\,, \ (P132) \\ &(P136) \quad \dot{Y}_i \supset Y_k Y_l \Gamma_{kl\to ij} - Y_i Y_j \Gamma_{ij\to kl}, \qquad \Gamma_{ij\to kl} = n_b \gamma_{ij\to kl}\,. \quad (P137) \end{aligned}$$

Here, the standard reaction rate $\gamma_{j\ldots\to i\ldots}$ is in units cm^3/s.

Based on (P136), one has for the transition from EGR to WIG (SIV):

$$\frac{dY_i}{d\tau'} = Y_k Y_l \Gamma'_{kl\to ij} - Y_i Y_j \Gamma'_{ij\to kl}, \Rightarrow \frac{1}{\lambda}\frac{dY_i}{d\tau} = Y_k Y_l \Gamma'_{kl\to ij} - Y_i Y_j \Gamma'_{ij\to kl},$$

where $d\tau' = \lambda\, d\tau$ based on the EGR↔WIG (SIV) relation $g'_{\mu\nu} = \lambda^2 g_{\mu\nu}$.

SIV analytic expressions [12]

The prefix "A" is used to indicate that the subsequent equation number refers to the corresponding original equation in ref. [12] ($\lambda = t_0/t$):

$$(A27) \qquad v_{eq} = K_0\, \rho_{\gamma 0}/(\Omega_m \rho_{c0})\,, \qquad c_2 = (v_{eq}^2 + \sqrt{v_{eq}^4 + C_{rel}})/t_{eq}^2\,, \quad (A21)$$

$$(A20) \qquad C_m = 4\Omega_m/(1-\Omega_m)^2, \qquad C_{rel} = C_m\, v_{eq}\,,$$

$$(A25) \qquad t_{eq} = 2^{-2/3}\left(v_{eq}^{3/2}(1-\Omega_m) + \sqrt{v_{eq}^3(1-\Omega_m)^2 + 4\Omega_m}\right)^{2/3},$$

$$(A29) \qquad t_{\text{in}} = C_{rel}^{1/4}/c_2^{1/2}\,, \qquad \Delta t = (t_0 - t_{\text{in}})\,\tau/\tau_0\,, \quad (A30)$$

$$(A33) \qquad a(\Delta t) = \sqrt{2c_2 t_{\text{in}}^3\,\Delta t}\,, \qquad \tau(T) = \frac{T_0^2\tau_0}{2(t_0 - t_{\text{in}})\sqrt{C_{rel}}}\frac{1}{T^2}, \quad (A39)$$

$$(A37) \qquad \rho_r(\Delta t) = \rho_{\gamma 0}\frac{K_0}{4C_{rel}\Delta t^2}\,, \qquad \rho_m(\Delta t) = \rho_{m0}\frac{c_2^{1/4}}{C_{rel}^{7/8}(2\Delta t)^{3/2}}.$$

Values of $a(T)$, $\tau(T)$, and $\rho(T)$ during the BBNS.

T [GK]	a(T)[10^{-9}]	SIV a(T)	t[s]	SIV τ[s]	$\rho_{\mathbf{tot2}}$	SIV$\rho_{\mathbf{rad}}$
9	0.218434	0.249208	1.24909	2.23615	287845.	92875.6
6	0.33151	0.373813	2.86926	5.03133	54801.9	18345.8
5	0.401382	0.448575	4.19779	7.24512	25683.6	8847.32
4	0.509668	0.560719	6.7449	11.3205	9997.75	3623.86
3	0.700877	0.747625	12.6701	20.1253	2856.65	1146.61
2	1.12735	1.12144	32.2898	45.282	445.583	226.491
1	2.61734	2.24288	168.002	181.128	16.4666	14.1557
0.9	2.95001	2.49208	212.491	223.615	10.2532	9.28756
0.8	3.35699	2.80359	274.024	283.013	6.1356	5.79818
0.7	3.86726	3.20411	362.272	369.649	3.49112	3.39879
0.5	5.44844	4.48575	714.557	724.512	0.887353	0.884732

Table 1: Values of $a(T)$, $\tau(T)$, and $\rho(T)$ for PRIMAT and SIV using standard cosmological parameters for $\Omega_{CDM}=0.26$, $\Omega_b=0.05$, and $h=0.677$. The PRIMAT $\rho_{\mathbf{tot2}}$ corresponds to the densities that use an effective number of neutrino flavors $N_\nu=3.01$. The densities ρ are in g/cm$^{\mathbf{3}}$.

The PRIMAT densities in the case of decoupled neutrinos:

$$\rho_\gamma = a_{BB}\left(k_B T\right)^4/c^2\left(1+\delta\rho(T)+\frac{7}{8}N_\nu\left(\frac{\langle T_\nu\rangle}{T}\right)^4\right)=T^4\bar{\rho}_\gamma,$$

$$\rho_m = \frac{n_{b0}m_{b0}}{c^2 a^3}\left(1+\Omega_{c0}/\Omega_{b0}+\frac{3}{2}k_B T/m_{b0}\right)=\frac{a_0^3\rho_{m0}(T)}{a^3}.$$

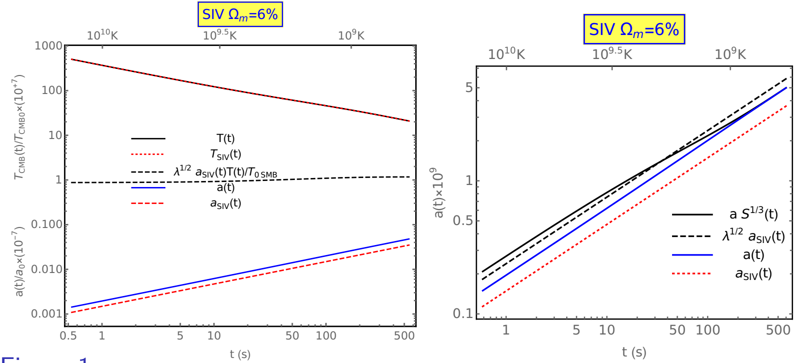

Figure 1: Expansion factor $a(t)$, $a(T)$, and temperature $T(t)$, along with the distortion $S(t)$ in $a(T)$ due to particle annihilations.

Conserved quantity within SIV: $a^{3(1+\omega)}\rho\lambda^{(1+3\omega)}$, where $\omega = p/\rho$.

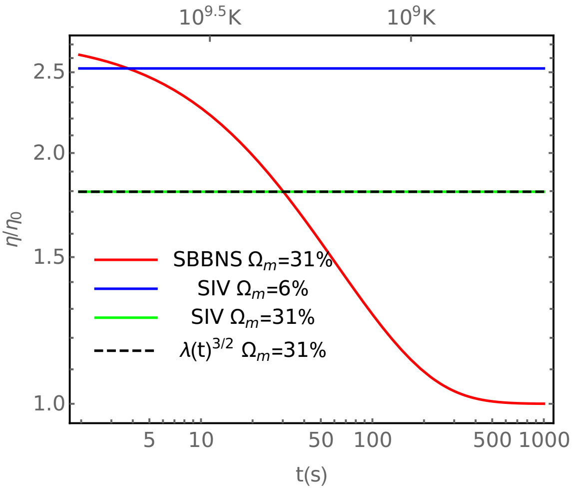

Figure 2: Baryon to photon ratio during BBNS.

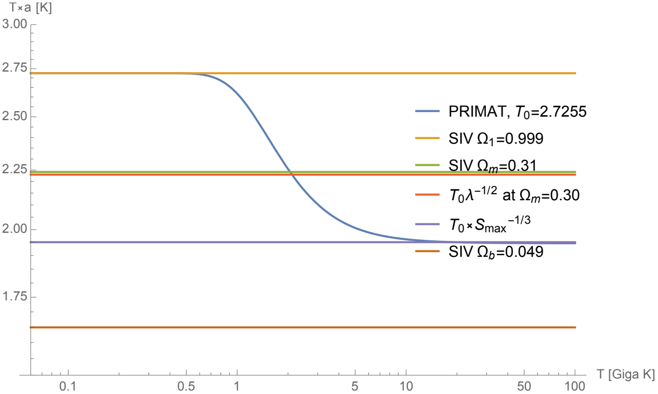

Figure 3: $T \times a(T) \to T_0$ for $\Omega_m = 0.999$ ($\lambda = 1$) coincides with PRIMAT's function at low $T < 1GK$. In agreement with $\lambda = 1/t_{\rm in} \to 1$ as $t_{\rm in} \to 1$ while $\Omega_m \to 1$. At high-temperatures ($T > 1GK$) PRIMAT $a(T)$ is smaller than the SIV for $\Omega_m = 0.31$, but bigger than the SIV case of $\Omega_m = \Omega_b = 0.05$. PRIMAT is running with $\Omega_m = 0.31$ and $\Omega_b = 0.05$; that is, $\Omega_{CDM} = 0.26$, but this value or any other nearby value do not have an impact on the BBNS within PRIMAT! The high-temperature ($T > 1GK$) regime in PRIMAT is due to the neutrino physics and e^+e^- annihilation. The high-temperature limit of $T \times a(T)$ for PRIMAT is based on the numerical value of the distortion factor $S(T) \to S_{max} = 11/4 \approx T_0$ at $T \gg 1GK$.

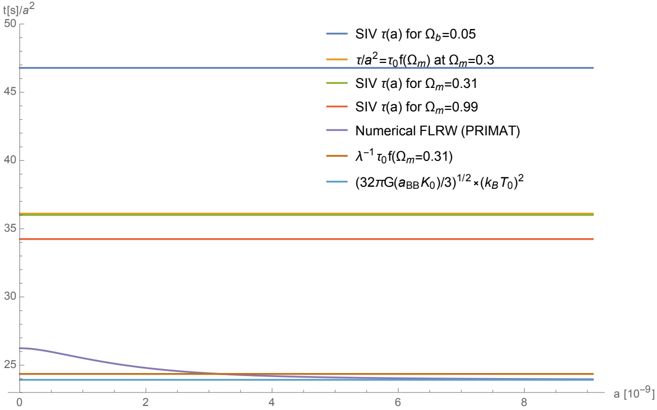

Figure 4: The SIV constant $\tau(a)/a^2$ is $\tau_0 f(\Omega_m)$. As it can bee seen $\tau(a)/a^2$ decreases with Ω_m but aways stays above the PRIMAT value. The gap between $\Omega_m = 1$ ($\lambda = 1$) and the PRIMAT $\tau(a)$ can be resolved by the λ–scaling of $8\pi G\rho$ as seen in the bottom curves. The bottom line is the asymptotic limit of $\tau(a)/a^2$ for PRIMAT based on the integration of $\sqrt{8\pi/3\,G\rho_{\gamma 0}}$ using the low-temperature radiation density limit for PRIMAT density ρ. The label on the vertical axes is set to be $t[s]/a^2$ in order to remind us that within PRIMAT time t is in seconds; thus, this $t[s]$ is not the SIV dimensionless time $t \in [0,1]$, but actually it is the $\tau[s]$ within the SIV since it is in seconds since the BB.

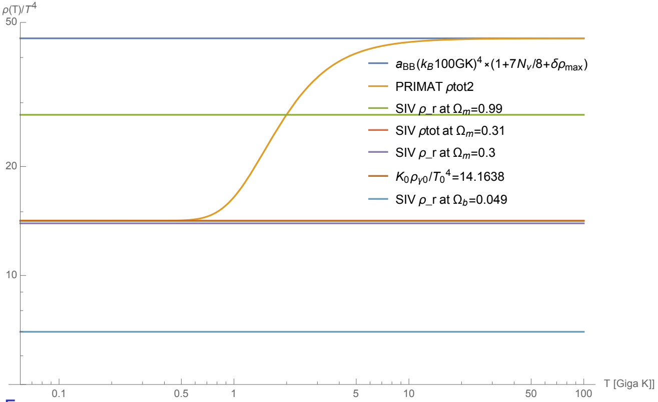

Figure 5: The $\rho(T)/T^4$ for SIV (ρ_{tot} and radiation ρ_r) at $\Omega_m = 0.999$ are below the PRIMAT $\rho(T)$ function at high temperatures ($T > 1GK$) due to the plasma corrections in this regime. The top line represents the high-temperature limit as evaluated at $N_\nu = 3$ and $\delta\rho_{max} \approx 1.742$ at $T = 100GK$. At low-temperatures ($T < 1GK$) PRIMAT $\rho(T)$ coincides with the SIV ρ_{tot} for $\Omega_m = 0.31$. It matches the value $K_0\rho_{\gamma 0}/T_0^4$. Note that $\Omega_m = 1$ is not realistic limit since the BBNS is in the radiation epoch but can be viewed as another way to say $\lambda = 1$. There are three lines near 14 that are very close and practically on top of each other.

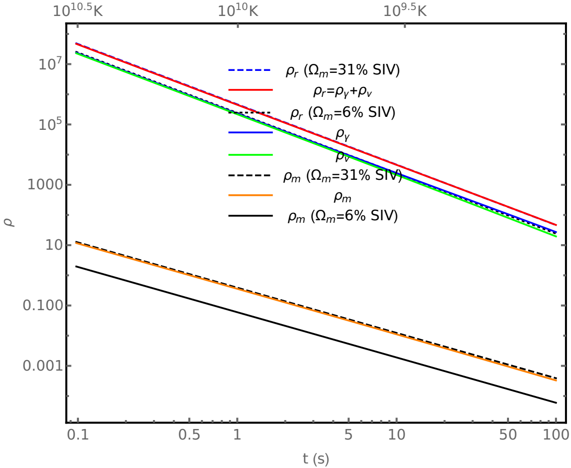

Figure 6: Relevant Energy-Densities, neutrinos, photons, both together as radiation, and matter densities during the Standard and SIV BBNS.

Element	Obs.	PRMT	a_{SIV}	fit	fit*	$\bar{a}/\lambda$	fit*	fit
H	0.755	0.753	0.805	0.755	0.849	0.75	0.753	0.755
$Y_P = 4Y_{\mathbf{He}}$	0.245	0.247	0.195	0.245	0.151	0.25	0.247	0.245
$\mathrm{D/H} \times 10^5$	2.53	2.43	0.743	2.52	2.52	1.49	2.52	2.53
$^3\mathrm{He/H} \times 10^5$	1.1	1.04	0.745	1.05	0.825	0.884	1.05	1.04
$^7\mathrm{Li/H} \times 10^{10}$	1.58	5.56	11.9	5.24	6.97	9.65	5.31	5.42
$N_{\mathbf{eff}}$	3.01	3.01	3.01	3.01	3.01	3.01	3.01	3.01
η_{10}	6.14	6.14	6.14	1.99	0.77	1.99	5.57	5.56
FRF	1	1	1	1	1.63	1	1	1.02
mŤ	1	1	1	1	0.78	1	1	0.99
Q/Ť	1	1	1	1	1.28	1	1	1.01
Ω_b [%]	4.9	4.9	4.9	1.6	0.6	1.6	4.4	4.4
Ω_m [%]	31	31	31	5.9	23	5.9	86	95
$\sqrt{\chi^2_\varepsilon}$	N/A	6.84	34.9	6.11	14.8	21.9	6.2	6.4

Table 2: The observational uncertainties are 1.6% for Y_P, 1.2% for D/H, 18% for T/H, and 19% for Li/H. FRF is the forwards rescale factor for all reactions, while mŤ and Q/Ť are the corresponding rescale factors in the revers reaction formula based on the local thermodynamical equilibrium. The SIV λ-dependences are used when these factors are different from 1; that is, in the sixth and ninth columns where FRF=λ, mŤ= $\lambda^{-1/2}$, and Q/Ť= $\lambda^{+1/2}$. The columns denoted by fit contain the results for perfect fit on Ω_b and Ω_m to ^{4}He and D/H, while fit* is the best possible fit on Ω_b and Ω_m to the ^{4}He and D/H observations for the model considered as indicated in the columns four and seven. The last three columns are usual PRIMAT runs with modified $a(T)$ such that $\bar{a}/\lambda = a_{SIV}/S^{1/3}$, where $\bar{a}$ is the PRIMAT's $a(T)$ for the decoupled neutrinos case. Column seven is actually $a_{SIV}/S^{1/3}$, but it is denoted by $\bar{a}/\lambda$ to remind us about the relationship $a' = a\lambda$; the run is based on Ω_b and Ω_m from column five. The smaller values of η_{10} are due to smaller $h^2\Omega_b$, as seen by noticing that η_{10}/Ω_b is always ≈ 1.25.

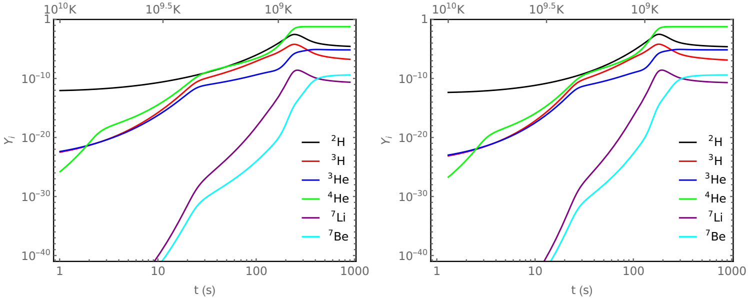

Figure 7: **Left: the Standard BBNS at $\Omega_{\rm m} = 31\%$. Right: SIV BBNS at $\Omega_{\rm m} = 6\%$**

Abundances of the light elements for modified T^{β} term in revers reaction formulas.

Element	Obs.	PRMT	a_{SIV}	λ^{0}	λ^{-1}	λ^{+1}	$\lambda^{1/2}$	$\lambda^{-1/2}$
H	0.755	0.753	0.805	0.755	0.755	0.755	0.755	0.755
Y_P=4Y_{He}	0.245	0.247	0.195	0.245	0.245	0.245	0.245	0.245
D/H $\times 10^{5}$	2.53	2.43	0.745	2.53	2.53	2.53	2.53	2.53
^{3}He/H $\times 10^{5}$	1.1	1.04	0.746	1.05	1.03	1.08	1.07	1.04
^{7}Li/H $\times 10^{10}$	1.58	5.57	11.9	5.24	5.66	4.81	5.02	5.45
N_{eff}	3.01	3.01	3.01	3.01	3.01	3.01	3.01	3.01
η_{10}	6.14	6.14	6.14	1.99	1.93	2.04	2.01	1.96
λ	1	1	1.	1.	2.43	2.76	2.66	2.5
m$\check{\text{T}}$	1	1	1.	1.	0.412	2.76	1.63	0.633
Ω_b [%]	4.9	4.9	4.9	1.6	1.5	1.6	1.6	1.6
Ω_m [%]	31	31	31	5.9	7	4.8	5.3	6.4
$\sqrt{\chi_{\varepsilon}{}^{2}}$	N/A	6.85	34.9	6.09	6.8	5.38	5.74	6.45

Table 3: Abundances of the light elements within the standard and SIV BBNS. The observational uncertainties are 1.6% for Y_P, 1.2% for D/H, 18% for T/H, and 19% for Li/H. The first five columns are the same as in Table 2 to facilitate the easy comparisons with the remaining columns. λ^{n} indicates the chosen scaling m$\check{\text{T}}$=λ^{n} for the temperature T^{β} in the revers reaction formulas. There is no rescaling of the forward reaction factors (FRF), nor for the $\exp(\gamma/T_9)$ factor, or any other temperature dependencies. The last five columns were fitted to reproduce ^{4}He and D/H.

Summary

- The **BBNS** within the SIV paradigm results in:
  - Compatible abundances to the standard BBNS at lower baryon and cold dark matter contend.
  - SIV-guided deviation from the local statistical equilibrium insensitivity of the T^β terms to the λ-scaling.
- Other research directions
  - * BBNS within the reparametrization invariance paradigm.
  - o Testing SIV cosmology against ΛCDM successes - CMB etc.

Summary

- The **BBNS** within the SIV paradigm results in:
  - Compatible abundances to the standard BBNS at lower baryon and cold dark matter contend.
  - SIV-guided deviation from the local statistical equilibrium insensitivity of the T^{β} terms to the λ-scaling.
- Other research directions
  - * BBNS within the reparametrization invariance paradigm.
  - o Testing SIV cosmology against ΛCDM successes - CMB etc.

Element	*Obs.*	*PRMT*	a_{SIV}	*fit*	*fit''*	$\bar{a}/\lambda$	*fit*	*fit'*	*fit**
H	0.755	0.753	0.805	0.755	0.813	0.776	0.766	0.749	0.755
$Y_P=4Y_{He}$	0.245	0.247	0.195	0.245	0.186	0.223	0.233	0.251	0.245
D/H x 10^5	2.53	2.43	0.743	2.52	2.57	1.07	2.6	2.6	2.53
^{3}He/H x 10^5	1.1	1.04	0.745	1.05	1.02	0.799	1.06	1.15	1.5
^{7}Li/H x 10^{10}	1.58	5.56	11.9	5.25	4.12	11.6	4.83	4.09	1.79
η10	6.14	6.14	6.14	1.99	2.58	6.14	4.71	7.49	12.5
λ	1	1	1.48	2.57	2.52	1.48	1.21	1.12	2.04
TRF	1	1	1.	1.	0.63	0.82	0.91	1.	0.91
m$\check{T}$	1	1	1.	1.	0.25	0.56	0.76	0.88	0.45
Q/$\check{T}$	1	1	1.	1.	0.63	0.82	0.91	0.88	0.54
Ω_b [%]	4.9	4.9	4.9	1.6	2.1	4.9	3.8	6	10
Ω_m [%]	31	31	31	5.9	6.3	31	57	71	12
$\sqrt{\chi_\varepsilon{}^2}$	1.	6.84	34.9	6.11	8.47	29.6	5.75	4.41	1.06
nT	0	0	0	0	−0.5	−1/2	−1/2	0	−0.13
nM	0	0	0	0	−1	−1	−1	−1.12	−1
η10SIV	6.14	6.14	1.9	0.117	0.646	3.42	3.56	5.34	1.94

Table 4: The observational uncertainties are 1.6% for Y_P, 1.2% for D/H, 18% for T/H, and 19% for Li/H. TFR is the temperature scaling factor, while m$\check{T}$ and Q/$\check{T}$ are the corresponding rescale factors in the revers reaction formula based on the local thermodynamical equilibrium. The SIV λ-dependences are used when these factors are different from 1; that is, TRF=λ^{nT} along with λ factor within $\sqrt{G\rho}$ The last four columns are usual PRIMAT runs with modified $a(T)$ such that $\bar{a}/\lambda = a_{SIV}/S^{1/3}$, where $\bar{a}$ is the PRIMAT's $a(T)$ for the decoupled neutrinos case. Column seven is actually $a_{SIV}/S^{1/3}$, but it is denoted by $\bar{a}/\lambda$ to remind us about the relationship $a' = a\lambda$.

References

[1] Weyl, H. 1923, Raum, Zeit, Materie. Vorlesungen über allgemeine Relativitätstheorie. Re-edited by Springer Verlag, Berlin (1970).

[2] Dirac, P. A. M. 1973, Proc. R. Soc. Lond. A, **333**, 403 (1973).

[3] Canuto, V., Adams, P. J., Hsieh, S.-H., & Tsiang, E., 1977, Phys. Rev. D **16**, 1643 (1977).

[4] Gueorguiev, V. G., Maeder, A., *Geometric Justification of the Fundamental Interaction Fields for the Classical Long-Range Forces.* Symmetry **13**, 379 (2021). e-Print: 1907.05248 [math-ph].

[5] Gueorguiev, V. G., Maeder, A., *The Scale Invariant Vacuum Paradigm: Main Results and Current Progress.* Universe 2022, **8** (4) 213; DOI:10.3390/universe8040213, e-Print:2202.08412 [gr-qc].

[6] Maeder, A. 2017, *An Alternative to the LambdaCDM Model: the case of scale invariance,* Astrophys. J. , **834**, 194 (2017). e-Print: 1701.03964 [astro-ph.CO].

[7] Maeder, A.; Gueorguiev, V.G. 2020, *The Scale-Invariant Vacuum (SIV) Theory: A Possible Origin of Dark Matter and Dark Energy,* Universe **6**, 46 (2020). DOI: 10.3390/universe6030046.

[8] Maeder, A.; Gueorguiev, V.G. *Scale-invariant dynamics of galaxies, MOND, dark matter, and the dwarf spheroidals,* MNRAS**492**, 2698 (2019). e-Print: 2001.04978 [gr-qc]

[9] Maeder, A., Gueorguiev, V., G., *The growth of the density fluctuations in the scale-invariant vacuum theory,* Phys. Dark Univ. **25**, (2019) 100315. e-Print: 1811.03495 [astro-ph.CO]

[10] Maeder, A., Gueorguiev, V. G., *Scale invariance, horizons, and inflation.* MNRAS **504**, 4005 (2021). e-Print: 2104.09314 [gr-qc].

[11] Pitrou, C., Coc, A., Uzan, J.-P., Vangioni, E. "Precision big bang nucleosynthesis with improved Helium-4 predictions." Physics Reports 754, 1–66 (2018). e-Print: 1801.08023.

[12] A. Maeder, "Evolution of the early Universe in the scale invariant theory," e-Print: 1902.10115.